BeBeC-2018-D26

COMPRESSED SENSING BASED RADIAL MODE ANALYSIS OF THE BROADBAND SOUND FIELD IN A LOW-SPEED FAN TEST RIG

Maximilian Behn, Benjamin Pardowitz and Ulf Tapken
German Aerospace Center (DLR), Institute of Propulsion Technology, Engine Acoustics Department
Müller-Breslau-Str. 8, 10623 Berlin, Germany

Abstract

A new inverse method for the radial mode analysis of the broadband sound fields in flow ducts is presented combining a Compressed Sensing approach and the eigenvalue decomposition of the sound pressure cross-spectral matrix. The Compressed Sensing method allows the accurate analysis of dominant modes by exploiting the block-structure of the radial mode spectrum and using sparse sensor arrays. The eigenvalue decomposition of the cross-spectral matrix is able to separate incoherent sound field constituents, which are sparse with respect to the in-duct modal spectrum and therefore are suitable for the Compressed Sensing approach. The application of the new method is demonstrated using measured data from a laboratory fan test-rig and the method is validated by comparison with results from a reference method using a full sensor array of 138 sensors. The method's potential to reduce the required number of sensors is evaluated by application of a reduced array with 34 sensors, by which the sound field is subsampled at high frequencies. The separation of incoherent sound field constituents by the eigenvalue decomposition is investigated in detail and its limitations are identified regarding the use of sparse arrays.

1 INTRODUCTION

The development of axial turbomachinery such as ventilators and aero engines imposes increasing requirements regarding the reduction of the broadband sound field components. Effective noise reduction technologies exist to reduce the tonal sound field components, which occur mainly at blade passing frequency and its harmonics. Technologies for substantial reduction of the broadband sound field components are subject of ongoing research. The experimental assessment of such technologies is typically made on the basis of measured sound power, for which numerous procedures exist in literature [1, 2, 5, 11]. Enghardt et al. [8] introduced a radial mode analysis technique, the FSA method, for the decomposition of

broadband sound fields into their mode constituents. This method was later reformulated by Jürgens et al. [10]. Recently, the application of the FSA method to determine broadband mode amplitudes for experimental data from a laboratory low-speed fan test rig was presented [18].

The main drawback of the FSA method is the large number of sensors that is required in order to perform the matrix inversion, which makes the method not feasible for application in large-scale fan test rigs. For the assessment of broadband mode analysis methods a laboratory fan test-rig was set up with a full sensor array consisting of 138 sensors. Attempts to reduce the required number of sensors are described by the authors in a previous study and are based on the incorporation of further assumptions on the sound field (cp. [18]). For instance, using a combination of a single ring equipped with 36 sensors and a line array equipped with 22 sensors the so-called CAAS (Combined Axial and Azimuthal Sensor Array) method determines the expected values of the squared mode amplitudes up to a frequency of 5000 Hz under the assumption that all modes are incoherent.

In this study the extension of a previously developed algorithm for in-duct radial mode analysis based on Compressed Sensing (CS-RMA) is investigated regarding the determination of the complete cross-spectral matrix of the mode amplitudes. The approach combines the analysis of mode sound power with the potential of Compressed Sensing to reduce the required number of sensors and the capability of the eigenvalue decomposition of the sound pressure cross-spectral matrix to separate incoherent sound field constituents, e.g. as shown by Suzuki and Day [15]. Compressed Sensing based mode analysis techniques have been introduced in literature with the aim to reduce the number of required sensors and to reconstruct sound fields consisting of more modes than the number of sensors, i.e. for subsampling sound fields. In the following, the method is validated by comparison with results of the FSA method. The accuracy of the method is evaluated based on the determined sound powers as well as the resulting mode coherences. Additionally, a reduced and optimized sensor array is used as input to the CS-RMA in order to investigate the method's potential to cope with subsampled sound field. The capability of the eigenvalue decomposition of the sound pressure cross-spectral matrix to separate incoherent sound field constituents is analyzed for the application of the full and the reduced array and its limitations are identified regarding the use of sparse arrays.

2 EXPERIMENTAL SETUP

The laboratory fan test rig is shown in Fig. 1 and was described in detail by Tapken et al. [18]. The test rig has an overall length of approximately 8 m. The main flow enters the test rig through a turbulence control screen (not shown in the figure) and a bellmouth nozzle at the inlet section. At the fan stage, the outer radius is 226.8 mm. The rotor of the low-speed axial fan stage has 18 blades and the stator consists of 32 vanes resulting in a cut-off design with respect to the first blade passing frequency. An anechoic termination is installed at the outlet section in order to minimize acoustic reflections. The mass flow and hence the aerodynamic operating condition of the rotor is adjusted by use of a throttle. The results given in the present study are calculated for a rotor speed of 3000 rpm and at operation conditions with a reduced mass flow $\dot{m}_{red} = 2.53$ kg/s and fan pressure ratio of $\pi = 1.0140$.

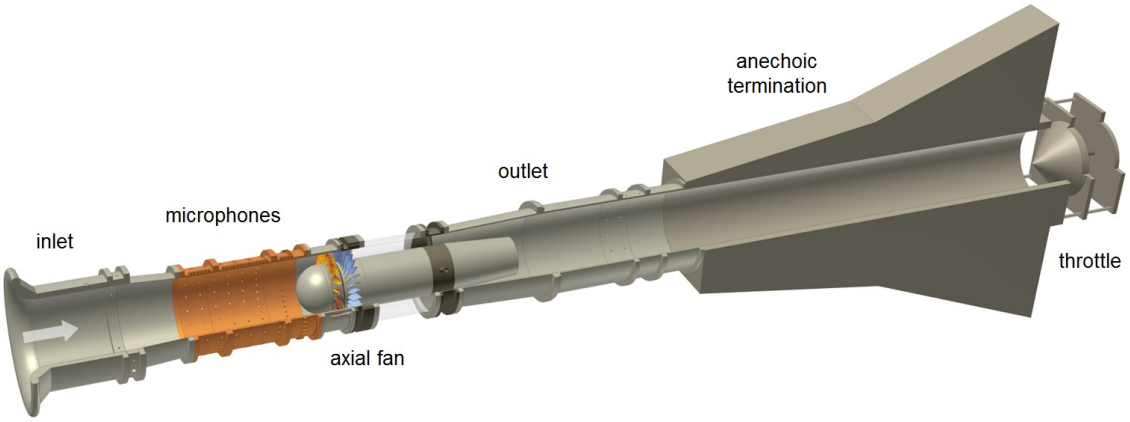

Figure 1: Overview of the experimental setup: Test rig with an axial fan stage in the center. Noise measurements are conducted by using sensor arrays consisting of wall-flush mounted microphones located upstream of the rotor (orange section).

The generated sound field is measured upstream of the axial fan stage with a reference microphone array consisting of 138 sensors. The microphone array section is illustrated in Fig. 2. The sensors are arranged in six uniform ring arrays at an axial spacing of 80 mm. Seen from the inlet, the first three rings are equipped each with 18 sensors, 24 sensors for rings 4 and 5 and 36 sensors for ring 6. Time series of the sound pressure signals with a measurement duration of 60 seconds were recorded at a sampling rate of 65.536 kHz.

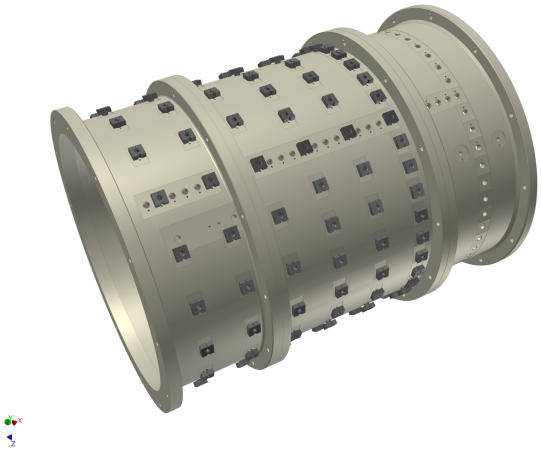

Figure 2: A sensor array consisting of 138 microphones distributed in six rings was used as input to the FSA method determining the reference results.

For further examination of the potential reduction of the number of sensors for the CS-RMA, a reduced sensor array is realized by selection of 34 sensor position from the reference microphone array. The optimal positions were determined by applying the optimization

procedure for non-uniform ring arrays as described by Behn et al. [3]. Figure 3 shows the resulting sensor array, where the first three rings are equipped each with 6 sensors and rings 4 and 5 are equipped each with 5 sensors. For ring 1 to 3 and 6 the same (optimal) sensor positions are chosen that were proven to be optimal as subset of the underlying sensor array consisting of 36 regularly spaced sensors. The approach of using a combination of optimized ring arrays for CS-RMA has been successfully applied at another test rig to the sound field generated by a single source [4], which in this case consists of fully correlated modes.

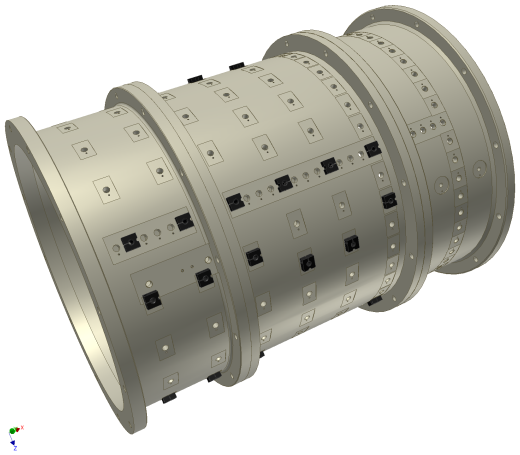

Figure 3: A reduced sensor array consisting of 34 microphones was designed by selecting optimal positions in the individual sensor rings from the full array depicted in Fig. 2.

3 RADIAL MODE ANALYSIS OF THE SOUND FIELD IN CIRCULAR FLOW DUCTS

The sound field in circular flow ducts is described by the superposition of an infinite number of modes, which are obtained from the general solution of the convective Helmholtz equation in cylindrical coordinates [19]:

$$p(x,r,\varphi) = \sum_{m=-\infty}^{+\infty} \sum_{n=0}^{+\infty} \left(A_{mn}^{+} \cdot e^{ik_{mn}^{+}x} + A_{mn}^{-} \cdot e^{ik_{mn}^{-}x} \right) e^{im\varphi} f_{mn}(r), \tag{1}$$

where incompressible and isentropic flow, a constant axial mean flow profile and stationary mean temperature and density are assumed. Here A_{mn}^{+} and A_{mn}^{-} denote the complex amplitudes, $f_{mn}(r)$ the radial mode shape function and k_{mn}^{+} and k_{mn}^{-} the axial wave numbers of the radial mode with azimuthal mode order m and radial mode order n propagating downstream and upstream. The radial mode shape factor is given by $f_{mn}(r) = (F_{mn})^{-1/2} \left(J_m(\sigma_{mn} r/R_o) + Q_{mn} Y_m(\sigma_{mn} r/R_o) \right)$ as a linear combination of the Bessel function of first respectively second kind and order m with associated eigenvalues σ_{mn} and Q_{mn}, which are obtained for hard-wall boundary conditions. R_o is the outer duct radius. The

eigenvalues depend on the duct geometry, i.e. the outer duct radius and the hub-to-tip ratio η. F_{mn} is a normalization factor [16].

In general, the radiated sound field of an axial fan stage exhibits tonal and broadband components, the first consisting of fully coherent modes and the latter being composed of modes of varying coherences. Both characteristics of the sound field can be modeled by a statistical description in terms of mean values and spatial cross-spectra. Therefore, the spatial cross-spectrum is determined for each combination of sensor positions (x,r,φ) and (x',r',φ') by the following equation:

$$S_{pp'} = \lim_{T\to\infty} E\left\{\frac{1}{T} p(\omega,x,r,\varphi) p^*(\omega,x',r',\varphi')\right\}. \tag{2}$$

The expectation value $E\{\ldots\}$ is approximated by time-averaging over a suitably long period [18]. From Eq. 1 and 2 the relation between the mode amplitudes and the resulting sound pressure signal at the microphone array is described in matrix notation as

$$\mathbf{S}_{pp} = \mathbf{W}\mathbf{S}_{aa}\mathbf{W}^H, \tag{3}$$

where $\mathbf{S}_{pp}$ is the cross-spectral matrix of the pressure signals, $\mathbf{S}_{aa}$ is the cross-spectral matrix of the mode amplitudes and $\mathbf{W}$ the mode transfer matrix with entries $w_{mn,\pm}(x,r,\varphi) = e^{ik^{\pm}_{mn}x} e^{im\varphi} f_{mn}(r)$.

The sound power $P^{\pm}_{mn}$ of the mode (m,n) transported in axial direction is calculated as [16]:

$$\left\langle P^{\pm}_{mn} \right\rangle = \frac{\pi R_o^2}{\rho c} \frac{\alpha_{mn}\left(1-M_x^2\right)^2}{\left(1\mp\alpha_{mn}M_x\right)^2} \left\langle \left|A^{\pm}_{mn}\right|^2 \right\rangle, \tag{4}$$

with the static density ρ, speed of sound c, the mode cut-on factor α_{mn} and the auto-power spectrum of the mode amplitude $\left\langle \left|A^{\pm}_{mn}\right|^2 \right\rangle$. By summation over all radial modes of the same azimuthal mode order the summed sound power transported in each direction is given as $\left\langle P^{\pm}_{m} \right\rangle = \sum_n \left\langle P^{\pm}_{mn} \right\rangle$. An additional summation over all azimuthal mode orders finally yields $\left\langle P^{\pm} \right\rangle = \sum_m \left\langle P^{\pm}_{m} \right\rangle$. From the determined cross-spectra of the mode amplitudes the mode coherences between two modes (m,n) and (μ,ν) is calculated as

$$C^{\mu\nu}_{mn} = \frac{\left|\langle A_{mn} A^*_{\mu\nu}\rangle\right|^2}{\langle |A_{mn}|^2\rangle \langle \left|A_{\mu\nu}\right|^2\rangle}. \tag{5}$$

3.1 Full Sensor Array (FSA) method

The Full Sensor Array (FSA) method is an inverse method, which determines the complete decomposition of broadband sound fields into all cut-on duct modes based on the cross-spectral

matrix of the sensor array. It was introduced in the context of in-duct radial mode analysis by Enghardt et al. [8] and later reformulated to the description given in the following by Jürgens et al. [10]. The FSA method was validated by application to various synthetic and experimental test cases and was proven to be very accurate and robust (see e.g. [8, 10, 17, 18]), thus serves for the current study as an established reference. A similar method was presented by Nelson and Yoon [12] for the estimation of acoustic source strengths. The FSA method solves Eq. 3 by making use of the pseudo-inverse $\mathbf{W}^{\dagger} = \left[\mathbf{W}^H\mathbf{W}\right]^{-1}\mathbf{W}^H$ according to following equation:

$$\mathbf{S}_{aa} = \mathbf{W}^{\dagger}\mathbf{S}_{pp}\left(\mathbf{W}^{\dagger}\right)^H. \tag{6}$$

3.2 Compressed Sensing based Radial Mode Analysis

In signal processing, Compressed Sensing is a framework for solving underdetermined systems of linear equations under the assumption that the solution vector is sparse [6]. In terms of the radial mode analysis this translates to the assumption that the mode spectrum features only a few dominant modes. Several mode analysis techniques on the basis of Compressed Sensing are described in literature (cp. [3, 4, 9, 20]), which allow the analysis of fully coherent, tonal sound field components. One point of interest is the analysis of the tonal components at blade passing frequency of axial fan stages, which exhibit strongly dominant modes of particular mode order [19]. The Compressed Sensing based radial mode analysis for fully coherent sound field components is based on the BOMP-algorithm [7] under the assumption that sound field components are composed of groups of dominant modes with the same azimuthal mode order. Grouping the mode amplitudes in a block vector $\mathbf{a}_{m,Block}$, whose elements are the sum over all radial modes of the same azimuthal mode order $\sum_{i=0}^{n_{max}(m)}\left(A_{mi}^{+}+A_{mi}^{-}\right)$, the method can be formulated in terms of a minimization problem as follows:

$$\underset{\mathbf{a}_{m,Block}\in\mathbb{C}^{N_{m,cut-on}}}{\operatorname{argmin}} \left\|\mathbf{a}_{m,Block}\right\|_1 \text{ subject to } \left\|\mathbf{p}-\mathbf{W}\mathbf{a}\right\|_2 < \varepsilon. \tag{7}$$

Here $N_{m,cut-on}$ denotes the number of unique azimuthal mode orders in the range of the propagating modes and ε is the assumed measurement noise energy. The BOMP-algorithm solves Eq. 7 by performing two fundamental steps iteratively: identification of the currently dominant azimuthal mode order and combined update of all dominant mode amplitudes, which were identified up to the current iteration. After each iteration the contribution of the dominant modes to the measured sound pressure signal is subtracted. All radial mode orders of the identified dominant azimuthal mode orders are determined at each iteration by inversion of a submatrix $\mathbf{W}_{m,Block}$ of the analysis matrix $\mathbf{W}$. Similar to the Compressed Sensing method for the azimuthal mode analysis (cp. [3]) the BOMP-algorithm is extended by a deconvolution step subsequently to the iterative determination of the dominant mode amplitudes enabling the estimation of the non-dominant modes in the case of strongly ill-conditioned or subsampled measurements and resulting in the complete mode amplitude vector $\mathbf{a}$.

In the present study, an extension of the method presented by Behn et al. [4] is investigated regarding its applicability to the analysis of broadband sound fields. First, the sound pressure cross-spectral matrix is decomposed into its coherent constituents by use of the eigenvalue

decomposition

$$\mathbf{S}_{pp} = \mathbf{U}\Lambda\mathbf{U}^H, \tag{8}$$

where $\mathbf{U}$ is a unitary matrix consisting of orthonormal eigenvectors $\mathbf{u}_i$ and Λ is a diagonal matrix with the corresponding eigenvalues λ_i with $i = 0, \ldots, N_{mic} - 1$. This follows from the fact that the cross-spectral matrix is positive semidefinite and Hermitian. Similar to the generalized inverse beamforming introduced by Suzuki [13, 14] the individual eigenvectors are weighted with their eigenvalue

$$\mathbf{v}_i = \sqrt{\lambda_i}\mathbf{u}_i \tag{9}$$

and used as input to the Compressed Sensing based radial mode analysis in Eq. 7 yielding the formulation of the Compressed Sensing method for the analysis of broadband sound fields:

$$\underset{\mathbf{a}_{m,Block_i} \in \mathbb{C}^{N_{m,cut-on}}}{\operatorname{argmin}} \|\mathbf{a}_{m,Block_i}\|_1 \text{ subject to } \|\mathbf{v}_i - \mathbf{W}\mathbf{a}_i\|_2 < \varepsilon. \tag{10}$$

Applying the BOMP-algorithm to Eq. 10 yields the mode spectra $\mathbf{a}_i$ corresponding to the eigenvalues λ_i. As a result, the cross-spectral matrix of the mode amplitudes is calculated by superposing the contributions of the individual coherent constituents:

$$\mathbf{S}_{aa} = \sum_{i=0}^{N_{mic}-1} \mathbf{a}_i \mathbf{a}_i^H. \tag{11}$$

3.3 Condition analysis of FSA method and the CS-RMA method

Due to the inversion of the Gram matrix $\mathbf{W}^H\mathbf{W}$ the FSA method is sensitive to the condition number $\kappa(\mathbf{W})$ (cp. Ref. [12]), which is shown for the full and the reduced array as a function of frequency in Fig. 4. Since during the iterative process of the BOMP-algorithm only submatrices of the analysis matrix $\mathbf{W}$ are inverted the CS-RMA method is less prone to errors caused by a large condition number. In general the condition is impaired close to the cut-on frequencies of the duct modes. The axial wavenumbers of modes close to their cut-on frequencies are generally very small and cause difficulties for the radial mode analysis procedure due to resulting minor phase differences of the respective mode components propagating down- and upstream. In the case of the reduced array, the non-uniform sensor positions induce additional correlations between each combination of cut-on modes [3] resulting in an increase of the condition number. The condition numbers of both arrays show small values of less than 10 up to about 1.3 kHz. At this frequency the modes $(\pm 1, 1)$ have their cut-on frequency. The largest peaks of the condition number are located at the cut-on frequencies of the mode orders $(\pm 2, 1)$, $(0, 2)$ and $(\pm 6, 0)$. In the case of the full array, the condition number increases steadily above the cut-on frequency of the mode $(0, 2)$.

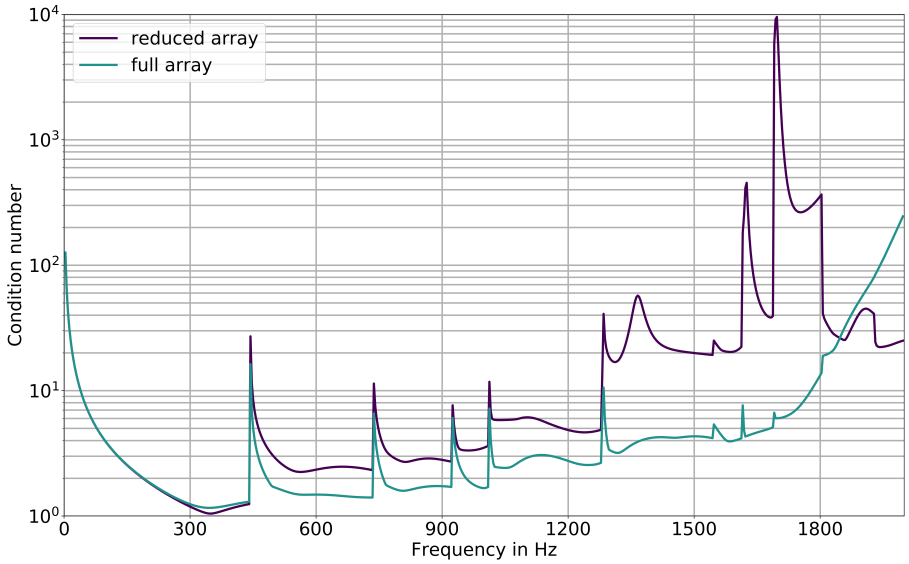

Figure 4: Condition number $\kappa(\mathbf{W})$ for the full and the reduced sensor array.

4 APPLICATION OF THE MODE ANALYSIS TECHNIQUES TO EXPERIMENTAL DATA

4.1 Verification of the Compressed Sensing based radial mode analysis

To investigate the accuracy of the CS-RMA method the method is applied to the full sensor array equipped with 138 sensors and the outcome of the method is compared to the reference, the FSA method. In Figure 5 the summed sound power for the upstream propagating modes generated by the axial fan and the reflected, downstream propagating modes are depicted. Peaks occur at the harmonics of the blade passing frequency (BPF) at 900 Hz and 1800 Hz and further in narrow- and broad-bands, which were found to be caused by the interaction of the rotor with incoming inhomogeneities of the turbulent flow field, the turbulent flow field interactions of rotor and stator and flow separations close to the rotor hub (cp. [18]). The results are identical up to a frequency of about 1.9 kHz, above which the increasing condition number (see Fig. 4) causes the deterioration of the accuracy of both methods.

Figure 6 shows the sound power of the upstream radiated modes with radial order $n = 0$ as outcome of the FSA and the Compressed Sensing method. The modal characteristics coincide very well, particularly for the dominant structures. The same agreement between the results of both methods is found for the comparison of the mode coherences of the radial modes of azimuthal mode order $m = 0$ with all other modes shown in Fig. 7. Tapken et al. [18] showed that only modes with the same azimuthal mode order are strongly correlated, whereas modes of different azimuthal mode orders have coherences close to zero as is indicated by the grey lines in Fig. 7. These findings support the assumption that the radial mode spectrum provides block-sparsity with respect to the azimuthal mode order, which is exploited by the BOMP-algorithm.

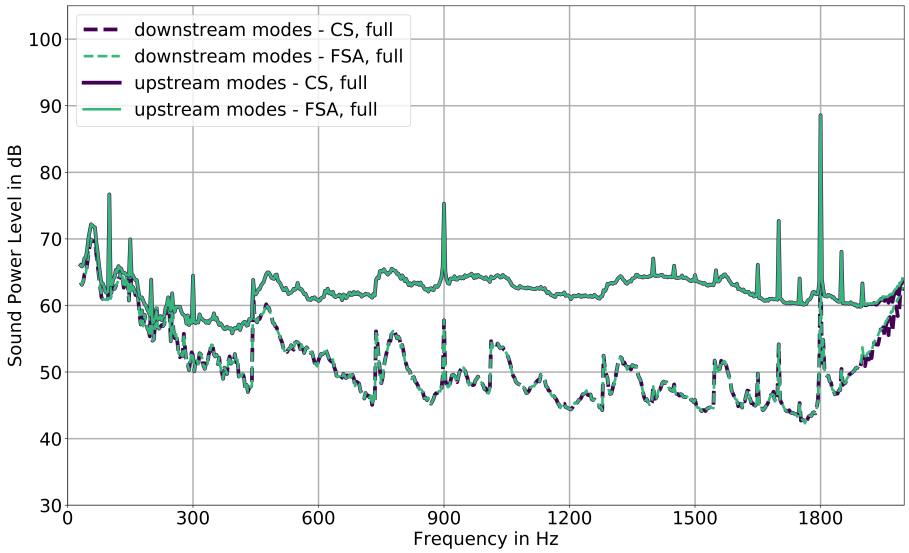

Figure 5: Verification of CS-RMA: Shown are the total sound powers determined using the FSA and the CS-RMA method, both applied to the full sensor array equipped with 138 sensors.

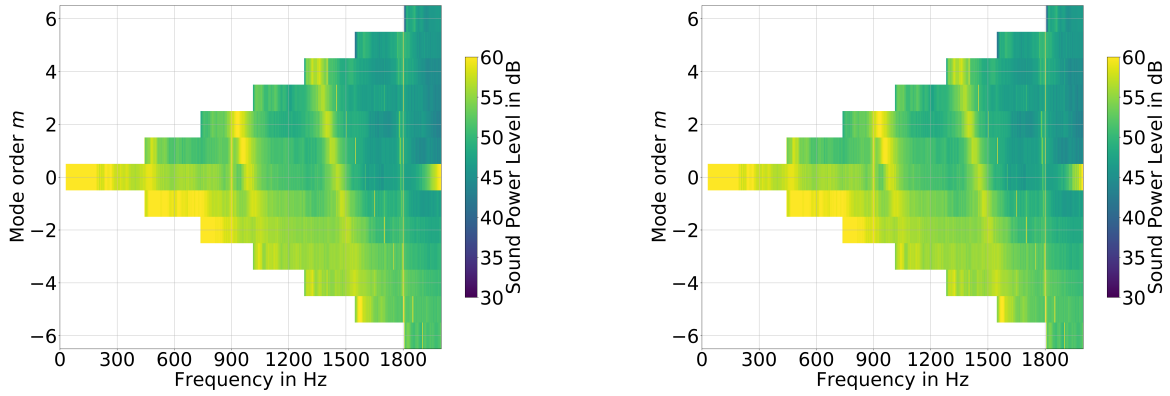

(a) FSA (b) CS

Figure 6: Comparison of the mode sound powers for radial mode order $n = 0$ determined using the FSA and the CS-RMA method, both applied to the full sensor array.

4.2 Application of the Compressed Sensing method using a reduced sensor array

In Figure 8 the summed sound power is depicted for the case the CS-RMA is applied to the reduced sensor array consisting of 34 sensors. The outcome is compared to the result of the FSA method in two variants: (i) FSA applied to the full array (138 sensors), (ii) FSA applied to the reduced array (34 sensors). At low frequencies below 400 Hz the results obtained with the reduced array are identical to the full array. Above the cut-on frequency of the radial modes $(\pm 1, 0)$ at approximately 450 Hz deviations from the reference results are found for

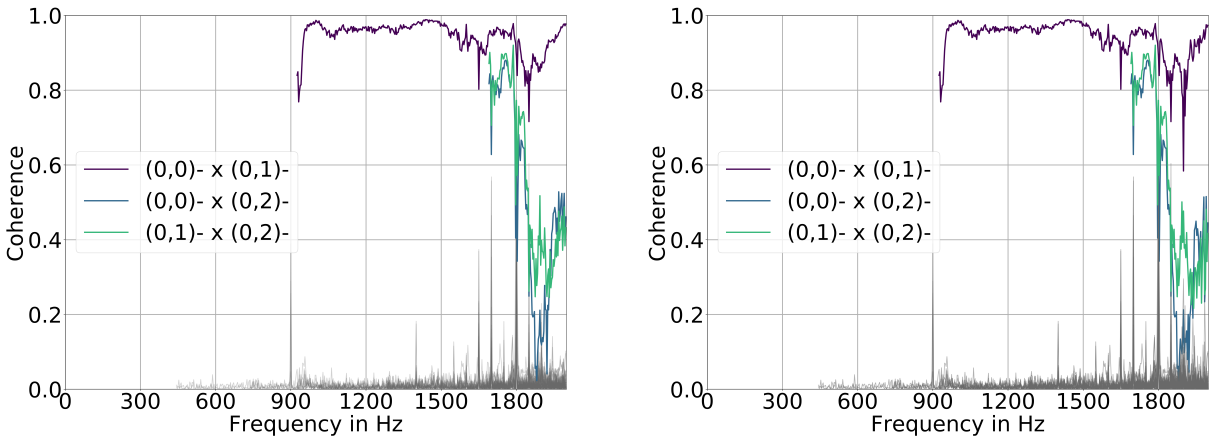

(a) FSA (b) CS

Figure 7: Comparison of the mode coherences of the radial modes of azimuthal mode order $m = 0$ with all other modes determined using the FSA and the Compressed Sensing method. Correlations of modes $m = 0$ with modes $m \neq 0$ are given by grey curves.

the reflected components, which increase in the vicinity of the cut-on frequencies of higher order modes. In general the results for the Compressed Sensing method determine the summed sound power of the radiated upstream modes accurately up to 1.9 kHz and overestimates the sound power of the reflected modes above 1.2 kHz. It should be noted that within the frequency range up to 2 kHz the maximum number of propagating modes is 44 and subsampling occurs above the cut-on frequency of the mode $(0,2)$ at 1.69 kHz. The application of the FSA method to the reduced array unexpectedly delivers almost the same results as the CS-RMA up to 1.5 kHz. However, at $f > 1.5$ kHz large deviations occur due to ill-conditioning of the system. The results presented here prove the minor sensitivity of the CS-RMA to the ill-conditioned analysis matrix $\mathbf{W}$ at high frequencies.

The mode sound powers of the upstream radiated modes with radial mode order $n = 0$ are shown in Fig. 9 using the reduced sensor array. Good agreement is achieved between the Compressed Sensing results and the reference results (FSA method, full array) in Fig. 9. Overall the spectral characteristics are detected almost identically for all modes. Towards 2 kHz the sound power level of the radial mode $(0,0)$ increases in the same way as the reference results, which is due to the limitations of the full sensor array. Despite the fact that the FSA method is not intended to be used with sparse sensor arrays the mode sound powers agree well up to 1.5 kHz between both methods.

The determined mode coherences of the modes of azimuthal mode order $m = 0$ with all other modes shown in Fig. 10 reveal increased differences to the reference results for both methods. The strength of the correlation between the modes of the same azimuthal mode order $m = 0$ is lower and the fluctuation over frequency is significantly increased in comparison to the reference results even in the frequency range, where the number of propagating modes is smaller than the number of sensors. Interestingly, the resulting mode coherences of both methods differ significantly in the frequency up to 1.5 kHz, whereas the mode amplitudes are

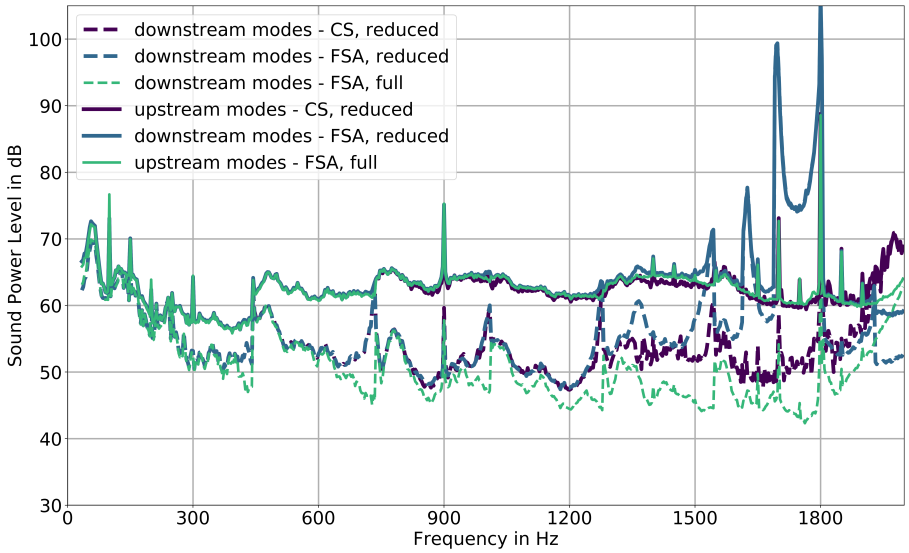

Figure 8: Comparison of the total sound power determined using the FSA and the Compressed Sensing method with the reduced sensor array. The results from the full array using the FSA method are considered as the reference.

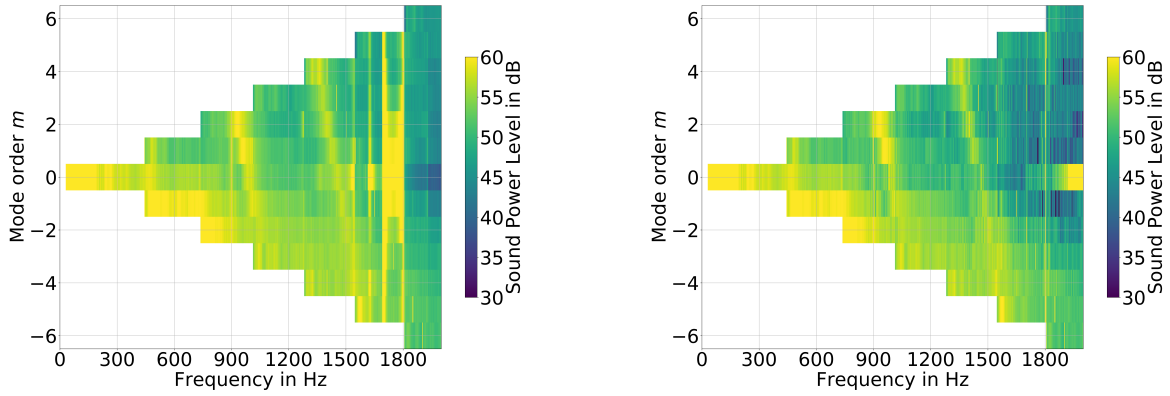

(a) FSA (b) CS

Figure 9: Comparison of the mode sound powers for radial mode order $n = 0$ determined using both the FSA and the Compressed Sensing method with the reduced sensor array.

in good agreement.

The deviations may be caused by the non-uniform sensor spacing and the resulting mutual coherence that is induced through the analysis matrix W [3]. The mutual coherence μ of the matrix $\mathbf{W}$ is defined as:

$$\mu(\mathbf{W}) = \max_{1 \le i < j \le N_{modes}} \frac{\left|\langle \mathbf{w}_i, \mathbf{w}_j \rangle\right|}{\|\mathbf{w}_i\|_2 \|\mathbf{w}_j\|_2}, \tag{12}$$

where $\mathbf{w}_i$ denotes the i-th column vector of the analysis matrix $\mathbf{W}$. With respect to the azimuthal

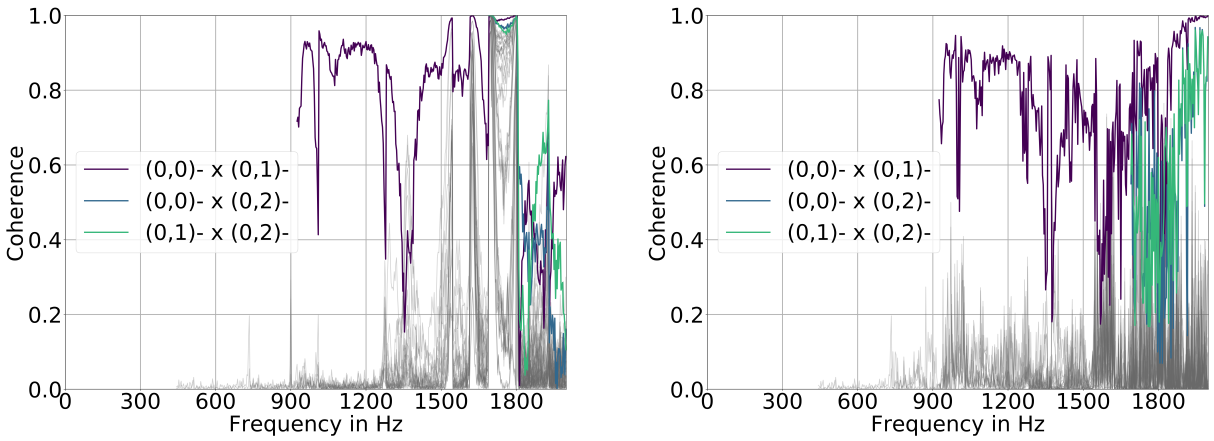

(a) FSA (b) CS

Figure 10: Comparison of the mode coherences of the radial modes of azimuthal mode order $m = 0$ with all other modes determined using the FSA and the Compressed Sensing method with the reduced sensor array.

mode decomposition the optimized ring arrays of the reduced array have a mutual coherence of 0.437 for rings 1,2,3 and 6 and 0.447 for rings 4 and 5. The resulting mutual coherence for the radial mode analysis is frequency-dependent and generally yields larger values than the mutual coherences of the single rings due to the influence of the axial wavenumber distribution of the radial modes.

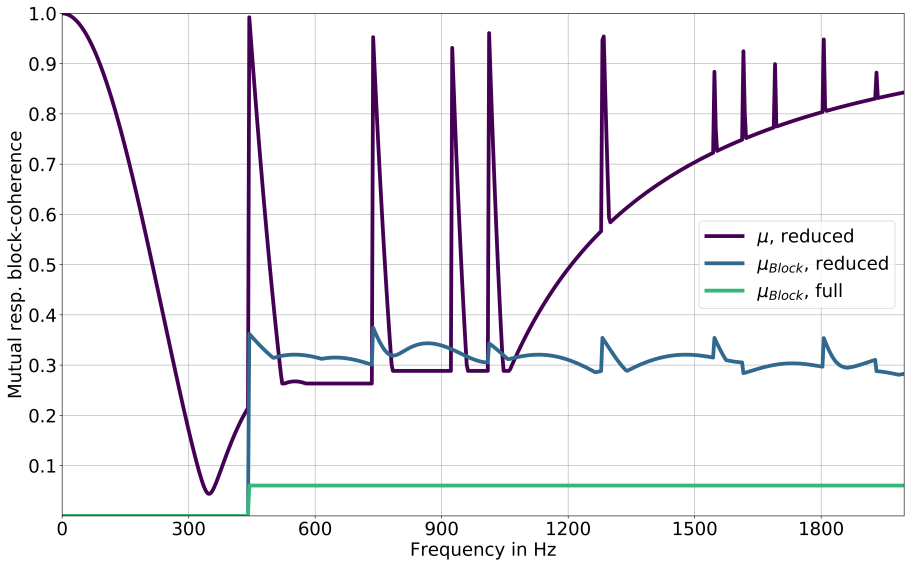

Figure 11: The block-coherence $\mu_{Block}(\mathbf{W})$ of the analysis matrix using the reduced and the full sensor array. The Mutual coherence $\mu(\mathbf{W})$ is given only for the reduced array.

Regarding the CS-RMA based on the BOMP-algorithm the block-coherence μ_{Block} [7] is

considered defined as:

$$\mu_{Block}(\mathbf{W}) = \max_{-|m_{max}|\leq s,t\leq|m_{max}|,\, s\neq t} \frac{1}{\sqrt{2\,(n_{max}(s)+1)\,2\,(n_{max}(t)+1)}} \lambda_{max}^{1/2}\left(\mathbf{W}_m(s)^H \mathbf{W}_m(t)\right), \tag{13}$$

where $\lambda_{max}\left(\mathbf{W}_m(s)^H \mathbf{W}_m(t)\right)$ denotes the largest eigenvalue of the resulting matrix from the product of submatrices $\mathbf{W}_m(s)^H$ and $\mathbf{W}_m(t)$ corresponding to the azimuthal mode orders s and t. Figure 11 shows block-coherence $\mu_{Block}(\mathbf{W})$ of the analysis matrix for the reduced array and the full array and the mutual coherence $\mu(\mathbf{W})$ in case the reduced array is applied. The mutual coherence is very sensitive at the cut-on frequencies of each radial mode and further indicates a relation to the development of the condition number due to the steady increase above 1 kHz. Above the cut-on frequency of the first higher azimuthal mode order the block-coherence yields values of about 0.3 resulting in the capability to determine the amplitudes of all radial modes of $s_{Block} < 1/\mu_{Block} \approx 3$ dominant azimuthal mode orders per eigenvector. The block-coherence of the full array yields values below 0.1 and is stable in the vicinity of the cut-on frequencies. The block-coherence of the reduced array is impaired close to the cut-on frequencies of each higher azimuthal mode orders, but is insensitive to the cut-on of higher radial mode orders.

The general improvement of the coherence when the block-structure of the radial mode spectrum is exploited supports the approach followed here for the CS-RMA. The authors believe that the frequency range of the analysis and the number of dominant modes, which is determined, can be extended despite of the low sensor count, if the positions for the sensor array optimization are completely free w.r.t. the axial and circumferential sensor positions. However, further investigation is necessary in order to profoundly understand the relationship between the analysis accuracy of the CS-RMA, the condition and the block-coherence of the analysis matrix.

It appears that the reconstruction of the mode coherences poses greater difficulties for the radial mode analysis with a reduced number of sensors than the reconstruction of the mode amplitudes. A possible reason for this may be found in the capability of the eigenvalue decomposition to separate incoherent modes, which is a key step in the mode analysis procedures for broadband sound fields in the current study.

5 EVALUATION OF THE CAPABILITY OF THE EIGENVALUE DECOMPOSITION FOR SEPARATING INCOHERENT MODES

The findings of the previous section raise the question, whether the eigenvalue decomposition of the cross-spectral matrix returns eigenvectors, which consist only of the contribution of correlated modes. If this is the case, the mode spectra corresponding to the individual eigenvalues are sparse and the CS-RMA is expected to have a high accuracy for the mode analysis.

In Figure 12 the mode spectra corresponding to the ten largest eigenvalues are plotted for the second blade passing frequency at 1800 Hz. The mode spectra are obtained by analysis of the individual weighted eigenvectors $\mathbf{u}_i$ for $i = \{1,\ldots,10\}$. Using the full array, the first

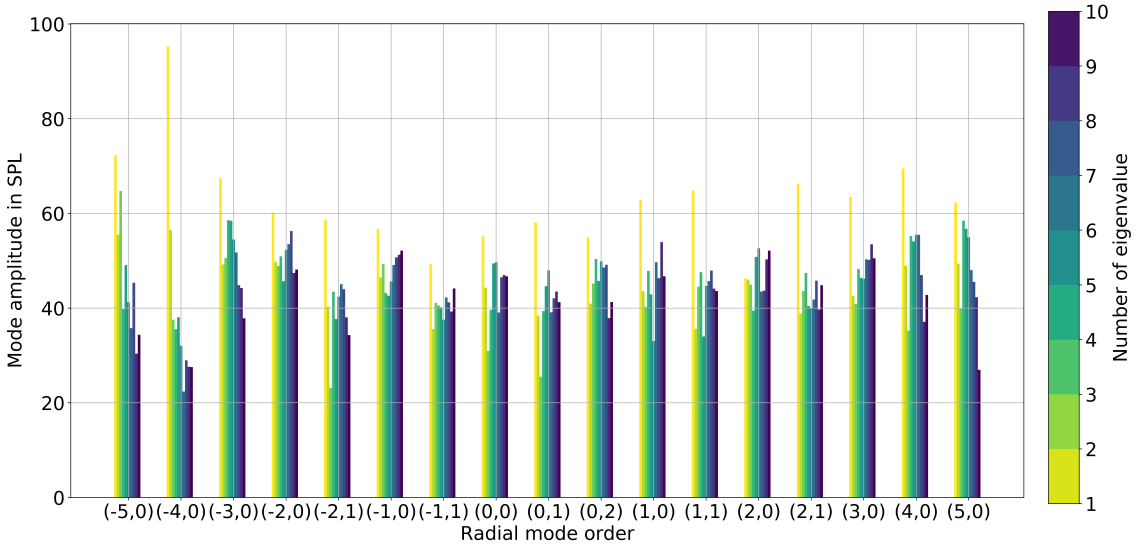

(a) FSA, full array, upstream radiated modes

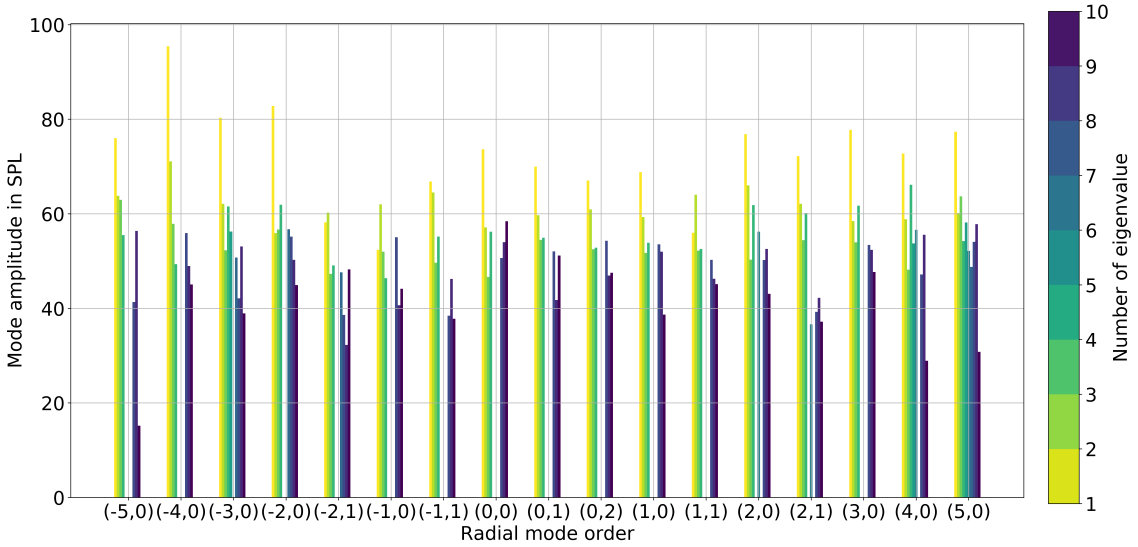

(b) CS, reduced array, upstream radiated modes

Figure 12: Comparison of the mode spectra corresponding to the ten largest eigenvalues at the second blade passing frequency of 1800 Hz determined using the FSA method with full sensor array and the Compressed Sensing method with the reduced sensor array.

eigenvalue is dominated by the contribution of the rotor-stator interaction mode of order $m = -4$. The following eigenvalues result in mode spectra, which yield levels much below the first eigenvalue and are not sparse. Interestingly, the interaction mode is the weakest mode in the mode spectra of the eigenvalues 3 to 10.

In case of the reduced array, the first eigenvalue for the analysis contains the contribution of the rotor-stator interaction mode and the resulting mode spectrum is similar to the FSA

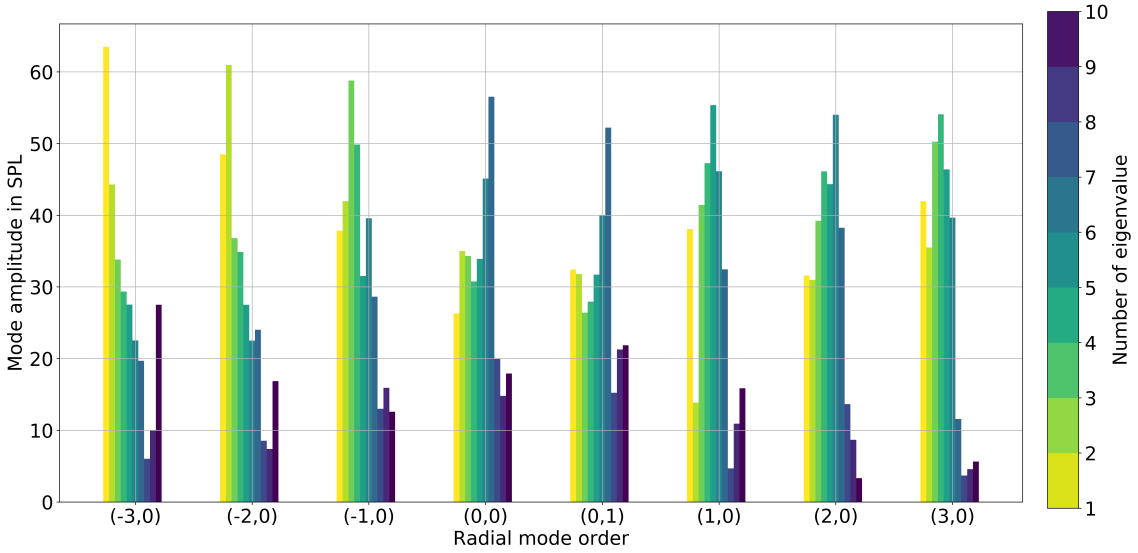

(a) FSA, full array, upstream radiated modes

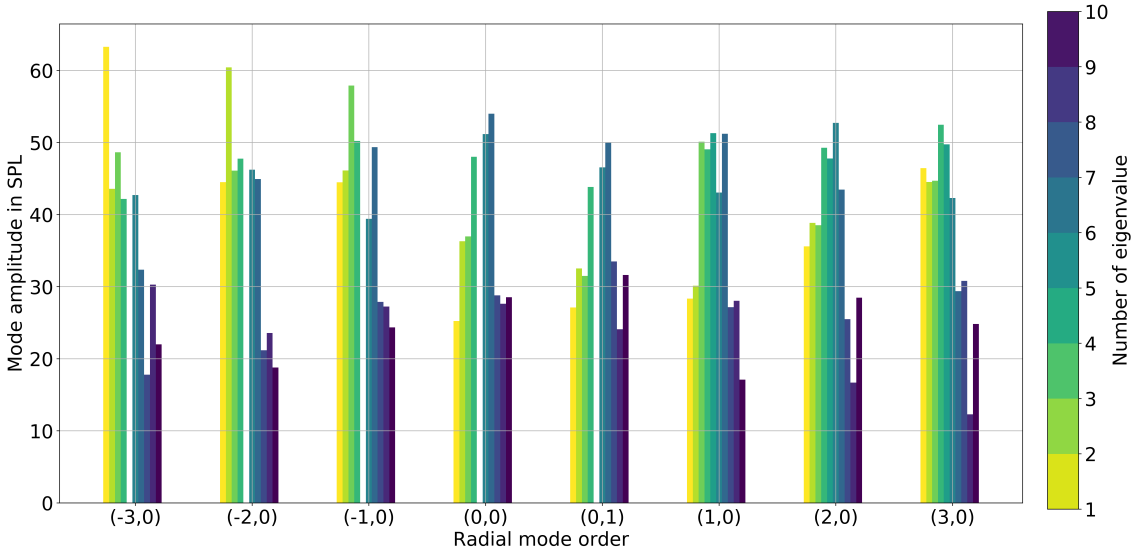

(b) CS, reduced array, upstream radiated modes

Figure 13: Comparison of the mode spectra corresponding to the ten largest eigenvalues at a broadband component of 1200 Hz determined using the FSA method with full sensor array and the Compressed Sensing method with the reduced sensor array.

method. At the second blade passing frequency the sound field is subsampled when the reduced array is used. The levels of the non-interaction modes, particularly mode $(-2, 0)$, are overestimated compared to the reference results. The individual mode spectra do not show contributions of all modes for each eigenvalue, which is a result of the iterative determination of the dominant modes and the subsequent estimation of the non-dominant modes in the Compressed Sensing method. The estimation of the non-dominant modes is not performed if

it has a significant impact on the amplitudes of the dominant modes. Nevertheless, it is proven that the eigenvalue decomposition successfully separates the dominant sound field due to the rotor-stator interaction mechanism and the other sound field constituents at the second blade passing frequency for both sensor arrays.

The analysis of the individual mode spectra for the ten largest eigenvalues at a broadband component of 1200 Hz is depicted in Fig. 14 exemplarily. The number of propagating modes is 16 and hence, the sound field is oversampled for both array configurations. Here the mode spectra corresponding to the first seven eigenvalues exhibit strong sparsity with only one or two dominant modes. In agreement to the observation in sec. 4 that the modes of azimuthal mode order $m = 0$ are strongly correlated, the modes $(0,0)$ and $(0,1)$ occur as dominant modes in the same eigenvalue using the FSA method and the full array. The mode spectra of eigenvalues 8 to 10 have very low levels of more than 20 dB below the mode $(0,1)$.

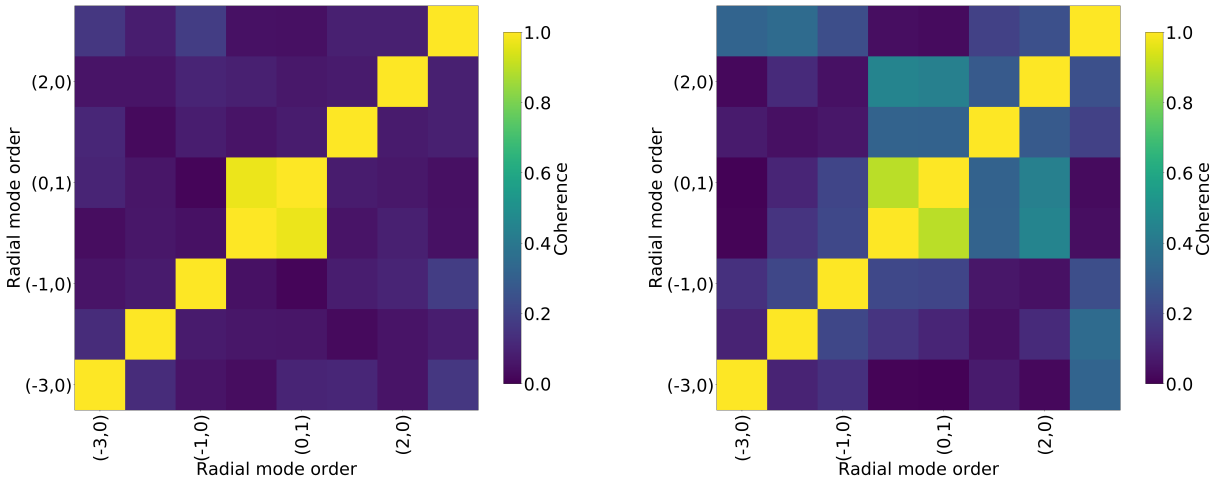

(a) FSA, full array

(b) CS, reduced array

Figure 14: Comparison of the mode coherences at a broadband component of 1200 Hz determined using the FSA method with full sensor array and the Compressed Sensing method with the reduced sensor array.

In case of the reduced array, only the first three eigenvalues yield mode spectra with strong sparsity, where the levels of the dominant modes $(-3,0)$, $(-2,0)$ and $(-1,0)$ each are almost identical to the results using the full array. The mode spectra of the following eigenvalues show significant contributions of all modes and indicate the incapability of the eigenvalue decomposition to separate the modes. This can diminish the accuracy of the mode analysis of both methods considered here, FSA and Compressed Sensing. Figure 14 presents the mode coherences between all cut-on modes at 1200 Hz for the configurations considered above, FSA using the full array and Compressed Sensing using the reduced array. For the first, it is identified that all modes of different azimuthal mode order are uncorrelated and only the modes of order $m = 0$ have a high coherence. For the latter, significant coherences occur for modes with different azimuthal mode orders, which is the result of the failing separation of the

incoherent modes by the eigenvalue decomposition. It is found that these observations hold also for the subsampled case at higher frequencies and hence, the limitations of the eigenvalue decomposition regarding the use in the CS-RMA are confirmed.

6 CONCLUSION

The present study introduces a new inverse method for the radial mode analysis of broadband sound fields in flow ducts combining a Compressed Sensing approach and the eigenvalue decomposition of the sound pressure cross-spectral matrix. It is shown by comparison with results from the reference method, the FSA method, that the CS-RMA gives very accurate results using a full sensor array with 138 sensors. The method allows the reconstruction of the complete cross-spectral matrix of the mode amplitudes and hence, enables the evaluation of mode sound power and mode coherences. The application of a reduced sensor array, which is selected from the full sensor array, reveals the good reconstruction of the mode sound power. The mode coherences in case the reduced array is applied show significant deviations from the reference results. A possible reason is the failing capability of the eigenvalue decomposition to separate the incoherent modes for over- and subsampled sound fields, if the mode spectrum does not feature particularly dominant modes. Further investigation of the relationship between the analysis accuracy of the CS-RMA and the characteristics of the applied sensor array is necessary. The identification of a different decomposition of the cross-spectral matrix in order to separate the incoherent sound field constituents and its incorporation into the CS-RMA is part of ongoing research.

References

[1] M. Åbom. "Modal Decomposition In Ducts Based On Transfer Functions Measurements Between Microphone Pairs." *Journal of Sound and Vibration*, 135(1), 95–114, 1989.

[2] F. Arnold. "Experimentelle und numerische Untersuchungen zur Schalleistungsbestimmung in Strömungskanälen." Reihe 7, nr. 353, Fortschrittsberichte VDI, 1999.

[3] M. Behn, R. Kisler, and U. Tapken. "Efficient Azimuthal Mode Analysis using Compressed Sensing." In *22nd AIAA/CEAS Aeroacoustics Conference, Lyon, France, May 30-June 01*. 2016.

[4] M. Behn, L. Klähn, and U. Tapken. "Comprehensive experimental investigation of mode transmission through stator vane rows: Results and calibration of an analytical prediction model." In *23rd AIAA/CEAS Aeroacoustics Conference, Denver, Colorado, June 05-09*. 2017.

[5] U. Bolleter and M. J. Crocker. "Theory and measurement of modal spectra in hard-walled cylindrical ducts." *Journal of the Acoustical Society of America*, 51, 1439–1447, 1972.

[6] D. L. Donoho. "Compressed Sensing." *IEEE Transactions on information theory*, 52(4), 1289–1306, 2006.

[7] Y. C. Eldar, P. Kuppinger, and H. Bölcskei. "Block-Sparse Signals: Uncertainty Relations and Efficient Recovery." *IEEE Transactions on signal processing*, 58(6), 3042–3054, 2010.

[8] L. Enghardt, A. Holewa, and U. Tapken. "Comparison of Different Analysis Techniques to Decompose a Broad-Band Ducted Sound Field in its Mode Constituents." In *13th AIAA/CEAS Aeroacoustics Conference, Rome, Italy, May 21-23*. 2007.

[9] X. Huang. "Compressive Sensing and Reconstruction in Measurements with an Aerospace Application." *AIAA Journal*, 51(4), 1011–1015, 2013.

[10] W. Jürgens, U. Tapken, B. Pardowitz, P. Kausche, G. J. Bennett, and L. Enghardt. "Technique to Analyze Characteristics of Turbomachinery Broadband Noise Sources." In *16th AIAA/CEAS Aeroacoustics Conference, Stockholm, Sweden, June 07-09*. 2010.

[11] E. J. Kerschen and J. P. Johnston. "A Modal Separation Measurement Technique for Broadband Noise propagating inside Circular Ducts." *Journal of Sound and Vibration*, 76(4), 499–515, 1981.

[12] P. A. Nelson and S. H. Yoon. "Estimation of Acoustic Source Strength by Inverse Methods: Part I, Conditioning of the Inverse Problem." *Journal of Sound and Vibration*, 233(4), 643–668, 2000.

[13] T. Suzuki. "Generalized Inverse Beam-forming Algorithm Resolving Coherent/Incoherent, Distributed and Multipole Sources." AIAA-2008-2954, 2008.

[14] T. Suzuki. "L1 generalized inverse beam-forming algorithm resolving coherent/incoherent, distributed and multipole sources." *J. Sound Vib.*, 330, 5835–5851, 2011. doi:10.1016/j.jsv.2011.05.021.

[15] T. Suzuki and B. J. Day. "Comparative study on mode-identification algorithms using a phased-array system in a rectangular duct." *Journal of Sound and Vibration*, 347, 27–45, 2015.

[16] U. Tapken and L. Enghardt. "Optimisation of sensor arrays for radial mode analysis in flow ducts." In *12th AIAA/CEAS Aeroacoustics Conference, Cambridge, Massachusetts (USA), May 08-10*. 2006.

[17] U. Tapken, D. Gutsche, and L. Enghardt. "Radial mode analysis of broadband noise in flow ducts using a combined axial and azimuthal sensor array." In *20th AIAA/CEAS Aeroacoustics Conference, Atlanta, Georgia, June 16-20*. 2014.

[18] U. Tapken, B. Pardowitz, and M. Behn. "Radial mode analysis of fan broadband noise." In *23rd AIAA/CEAS Aeroacoustics Conference, Denver, Colorado, June 05-09*. 2017.

[19] J. Tyler and T. Sofrin. "Axial Flow Compressor Noise." *SAE Transactions*, 70, 1962.

[20] W. Yu and X. Huang. "Compressive sensing based spinning mode detection by in-duct microphone arrays." *Measurement Science and Technology*, 27(5), 2016.